Fabrication of Inorganic/Polymer Nanocomposite Membranes Containing Very High Silica Content via *In Situ* Surface Grafting Reaction and Reactive Dispersion of Silica Nanoparticles: Proton Conduction, Water Uptake, and Oxidative Stability

Ju-Young Kim,[1] Young-Hwan Ohn,[1] Kyo-Jin Ihn,[2] Changhyun Lee[3]

[1]*Department of Advanced Materials Engineering, College of Engineering, Kangwon National University, Samcheok, Gangwon-Do 245-711, South Korea*
[2]*Department of Chemical Engineering, College of Engineering, Kangwon National University, Chunchon, Gangwon-Do 200-701, South Korea*
[3]*Macrmolecules and Interfaces Institute and Chemistry Department, Virginia Polytechnic Institute and State University, Blacksburg, Virginia 24601*

Received 27 January 2010; accepted 26 May 2010
DOI 10.1002/app.32939
Published online 25 August 2010 in Wiley Online Library (wileyonlinelibrary.com).

ABSTRACT: In this study, we present a new fabrication process for proton exchange membranes based on inorganic/organic nanocomposite using *in situ* surface grafting reaction and reactive dispersion of silica nanoparticles in the presence of reactive dispersant, urethane acrylate nonionomer (UAN). Through *in situ* surface grafting reaction of silica nanoparticles, urethane acrylates were chemically introduced on the surface of silica nanoparticles, which were dispersed in DMSO solutions containing UAN and sodium styrene sulfonate (NaSS). After urethane linkage and copolymerization of NaSS, UAN and urethane acrylate moieties of silica nanoparticles, the solutions were converted to silica nanoparticle-dispersed proton exchange membranes where silica particles were chemically connected with organic polymer chains. 5.89–29.45 wt % of silica nanoparticles could be dispersed and incorporated in polymer membranes, which were confirmed by transmittance electron microscopy (TEM) measurement. On varying weight % of silica nanoparticles dispersed within the membranes, water uptake and oxidative stability of nanocomposite membranes were largely changed, but membranes showed almost the same proton conductivity (greater than 10^{-2} S cm^{-1}). At 5.89 wt % of silica nanoparticles, nanocomposite membranes showed the lowest water uptake and excellent oxidative stability compared to the sulfonated polyimide membranes fabricated by us. © 2010 Wiley Periodicals, Inc. J Appl Polym Sci 119: 2002–2009, 2011

Key words: silica; nanoparticles; proton exchange membranes; nanocomposites

INTRODUCTION

The proton exchange membrane (PEM) is one of major elements in solid-typed fuel cells such as proton exchange membrane fuel cell (PEMFC) and direct methanol fuel cell (DMFC). A successful PEM should maintain these functions under a variety of operating conditions and over the entire life of the fuel cells. Nafion® has been recognized as a highly capable material owing to its high proton conductivity and excellent chemical and mechanical durability. Because of high cost and methanol permeability of Nafion, a great deal of research has focused on the development of low-cost alternatives that have excellent proton conductivity even at high temperature or low humidity.[1–3] Currently, many research groups have reported the fabrication of proton conducting membranes containing inorganic oxides such as SiO_2, TiO_2, or ZrO_2 to improve chemical and mechanical properties, as well as proton conductivity of polymeric membranes.[4–6] In most of cases, inorganic oxides were incorporated into the polymer matrix using sol-gel process of inorganic precursors such as tetraethoxysilane (TEOS), titanium(IV)*n*-butoxide, zirconium *n*-butoxide, etc.[4–12]

At our preceding reports,[13,14] we presented fabrication of nanocomposite proton exchange membrane where silica nanoparticles were nanodispersed by aid of amphiphilic reactive dispersant, urethane acrylate nonionomer (UAN) which has polypropylene-based hydrophobic segment and polyethylene oxide-based hydrophilic segment at the same backbone and has reactive vinyl groups located at both ends of its polypropylene-based hydrophobic segment. UAN chains could not only increase dispersibility of silica nanoparticles but also be copolymerized with several monomers to form membranes

Correspondence to: J.-Y. Kim (juyoungk@kangwon.ac.kr).

having nanophase-separated structure. Sulfonated polyimide and sulfonated poly(urethane acrylate-*co*-styrene) membranes containing nanodispersed silica nanoparticles by aid of UAN chains exhibited improved hydrolytic and chemical stability and reduced methanol permeability.[13,14]

Even though improved mechanical properties of the membranes could be achieved by incorporating 1–2 wt % of silica nanoparticles, the maximum amount of silica nanoparticles dispersed in the membranes using UAN was less than 3 wt %. In this study, we present a new fabrication process for inorganic/organic nanocomposite membranes containing high silica nanoparticle content (higher than 5 wt %) for highly improving chemical and thermal stability of polymeric membranes. That is, *in situ* surface-grafting of silica nanoparticles, stabilization of dispersed silica nanoparticles and formation of nanocomposite membrane were carried out simultaneously in the same medium to maximize amounts and dispersibility of silica nanoparticles in the membrane.

In this article, fabrication of silica/polymer nanocomposite membranes through a novel curing process was first presented. Nanocomposite membranes having various weight % of silica nanoparticles were fabricated to investigate the effect of dispersibility and content of silica nanoparticles on chemical stability, proton conductivity, water uptake, and thermal stability of the membranes. Nanostructure of fabricated nanocomposite membranes was also investigated using transmittance electron microscopy (TEM) measurements, and discussed it in relation to their properties.

EXPERIMENTAL

Materials

In the synthesis of UAN chain, glycerol propoxylate (PPO triol, MW = 1000, Aldrich Chemical, WI), 2,4-toluene diisocyanate (TDI, Aldrich Chemical, WI), 2-hydroxyethyl methacrylate (2-HEMA, Aldrich Chemical, WI), and polyethylene glycol (PEG, MW = 1500, Aldrich Chemicals, WI) were used. PPO triol and PEG were dried and degassed at 80°C and 3–5 mmHg for 2 days. Styrene, sodium styrene sulfonate (NaSS), dibenzoyl peroxide (BPO), and dimethyl sulfoxide (DMSO) were purchased from Aldrich Chemical (WI) and were used as received. Nanosilica powders, Aerosil® 200 (Hydrophilic nanosilica powder, average primary particle size = 12 nm) were purchased from Degussa Chemicals (Dusseldorf, Germany) and were dried at 80°C and 3–5 mmHg before use.

Synthesis of UAN

UAN used in this study as a reactive dispersant was synthesized through an established three-step process with a constant molar ratio of TDI/PPO triol/2-HEMA/PEG (3/1/2/1).[15,16] The average molecular weight of the synthesized UAN was 6700 with a polydispersity of 2.01. Molecular structure of UAN chain is schematically presented at Figure 1.

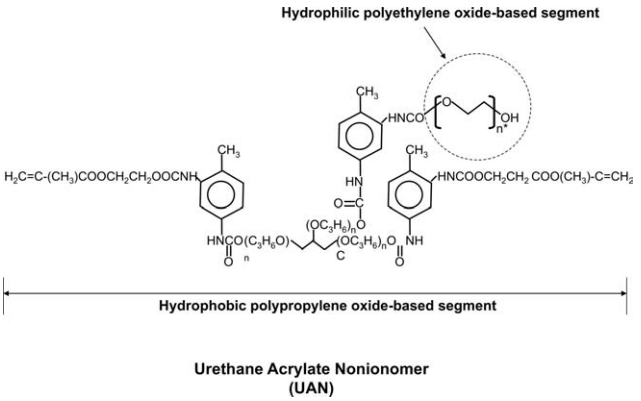

Figure 1 Schematic presentation of chemical structure of UAN (n = 5.22 and n^* = 29.25–35.84 calculated based on molecular weight provided by Aldrich Chemical).

Fabrication of organic membranes

As presented in Table I, 12.1 g of TDI were reacted with 18.3 g of HEMA in 10 g of DMSO for 3 h at room temperature. Then, 7.5 g of NaSS and 10.0 g of UAN were added and dissolved to form homogeneous solution. Finally, radical initiator, AIBN was added to the mixtures and poured into a silicone-packed mold to carry out crosslinking copolymerization for 3–4 h at 70°C to obtain wall-to-wall membranes with 150 μm thickness. Obtained membranes were immersed at water acetone mixture for 24 h for purification and then dried for 2 days. Before proton conductivity, water uptake, thermal and oxidative stability measurements, sodium ions of membranes were exchanged for protons by immersion in 0.5 M H_2SO_4 for 2 days, followed by rinsing and washing with deionized water several times. Obtained poly(styrene-NaSS-UAN) random copolymer membranes were named as PSSU membranes.

Fabrication of silica/polymer nanocomposite membranes

Silica/polymer nanocomposite membranes were fabricated using three-step process: (1) introduction of isocyanate groups onto the silica surface, (2) introduction of urethane acrylate onto the silica surface and synthesis of urethane acrylate, and (3) radical copolymerization and urethane linkage. These reactions were carried out consecutively and continuously at the same reaction solution.

1st step: Introduction of isocyanate groups onto the silica surface

To introduce isocyanate groups onto the silica surface through the reaction between NCO groups of

TABLE I
Recipe for the Fabrication of Nanocomposite Membranes

Sample	Ingredients						
	Aerosil 200 (g)	TDI (g)	HEMA (g)	UAN (g)	NaSS (g)	DMSO (g)	Silica (wt %)
PSSU	0.00	1.22	1.82	1	0.72	10	0
SSUH-1035	0.30	1.74	1.30	1	0.75	11	5.89
SSUH-1100	1.00	1.74	1.30	1	0.75	14	17.27
SSUH-1125	1.25	1.74	1.30	1	0.75	16	20.69
SSUH-1150	1.50	1.74	1.30	1	0.75	18	23.85
SSUH-1200	2.00	1.74	1.30	1	0.75	25	29.45

TDI and silanol groups of silica particle, 3.0–20 g of Aerosil® 200 nanosilica powders (1.37 mmol/g of silanol groups)[17,18] were first mixed with DMSO using ultrasonication at room temperature for 0.5 h. Then, 17.4 g (100 mmol) of TDI and 10 mg of DBTDL were dissolved and reacted for 3 h at room temperature. Since the number of NCO groups was much larger than that of silanol groups in the reaction solution, most of NCO groups remain unreacted even after complete reaction between NCO groups and silanol groups.

2nd step: Introduction of urethane acrylate onto the silica surface and synthesis of urethane acrylate

13.0 g of 2-HEMA (100 mmol) was added at the prepared solution and the reaction was carried out at room temperature for over night to introduce urethane acrylate onto silica surface through the reaction between OH groups of 2-HEMA and NCO groups introduced onto the silica surface through 1st step. At the same time, added 2-HEMA reacted with NCO groups of TDI molecules which were not reacted with silanol groups of silica surface, resulting in formation of urethane acrylate molecules which were not chemically bound with the silica particles.

3rd step: Radical copolymerization and urethane bridging

10 g of UAN, 7.5 g of NaSS, and 0.05 g of BPO were added in the prepared solution and mixed at room temperature. After complete dissolving, the reaction solutions were poured into a silicon-packed mold (5 cm × 5 cm × 150 μm) for fabrication of nanocomposite membrane. The molds containing the reaction solutions were left in 80°C oven for 4 h to carry out radical initiated copolymerization and urethane bridging. After completion of curing process, obtained membranes were immersed in water–acetone mixture (24 h) for purification and then dried for 2 days at 80°C. Before measuring the membrane performance, the membranes in the sodium salt form were acidified into the protonated form by immersion in 0.5 *M* H_2SO_4 for 2 days, followed by rising and washing with deionized water several times. The resultant membranes were denoted as SSUH membranes. Recipe for fabrication of membranes were summarized at Table I.

Water uptake and proton conductivity measurement

The water uptake of the membranes was measured after immersing each membrane into deionized water at 30°C for 24 h. The membranes were then removed, wiped with tissue paper, and immediately weighed on a microbalance. The water uptake (W) of the membranes was expressed as follows:

$$W = \frac{(W_{\text{wet}} - W_{\text{dry}})}{W_{\text{dry}}} \times 100\ (\%) \qquad (1)$$

where W_{dry} and W_{wet} are the weight of the dry and the corresponding water-sorbed membranes, respectively. The water uptake of the SSUH membranes was calculated from the average value of W for five membrane coupons. The proton conductivity of each membrane coupon (1.0 cm width × 4.0 cm length) was measured using an electrode system connected with a frequency response analyzer (Solatron 1260) and an electrochemical interface (Solatron 1287, Farnborough Hampshire, ONR, UK). The four-point probe alternating current (ac) impedance spectroscopic technique was used to eliminate the inductive impedance caused by the electric conductive leads and the potentiometer.[19,20] The electrode system was placed in a thermohumidity controlled chamber to measure the proton conductivity at constant humidity (95% relative humidity (RH)) and temperature (60°C). Using this method, a fixed ac current is passed between two outer electrodes, and the resistance of the membrane is calculated from the ac potential difference between the two inner electrodes. The proton conductivity was obtained using the following equation:

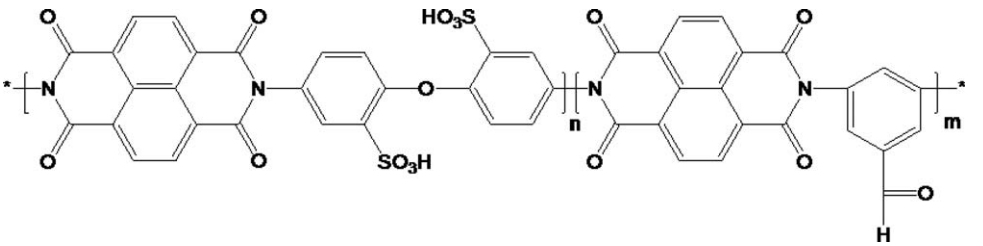

Figure 2 Basic chemical structure of sulfonated polyimide used as a reference in this study ($n = 0.4$ and $m = 0.6$).

$$\sigma = \frac{L}{(R \times S)} \tag{2}$$

where σ is the proton conductivity (S cm^{-1}), L is the membrane thickness (cm), R is the resistance (Ω), and S is the effective membrane surface area for proton migration (cm^2).

Membrane characterization

The oxidative stability to peroxide radical attack was investigated by measuring the elapsed times that a membrane began to dissolve or when the membrane was broken or lightly bent (τ_1), and a membrane was dissolved completely (τ_2) after immersion of each membrane into Fenton's reagent of the 30 wt % H_2O_2 and 0.1 wt % ferrous ammonium sulfate solution at 80°C.[21–23] Thermal stability of the membranes was measured using thermogravimeric analyzer (TGA) (TA Instrument TGA 2050, New Castle, DE). TGA measurements were carried out under nitrogen atmosphere with a heating rate of 10°C from 20 to 700°C. For comparing oxidative stability, the sulfonated polyimide (SPI; Ion exchange capacity = 1.90 meq g^{-1}) with the chemical structure illustrated at Figure 2 was synthesized by solution-thermal imidization method, using 4′,4′-diaminodiphenyl ether 2,2′-disulfonic acid (SODA, 1.6 mmol), 3,5-diaminobenzoic acid (DBA, 2.4 mmol), and 1,4,5, 8-naphthalenetetracarboxylic dianhydride (NTDA, 4 mmol). Detail synthetic protocol was described in our published references.[20,24] Also the SPI has about 33% of water uptake and 6.5×10^{-2} S cm^{-1} of proton conductivity at 30°C and 90% RH.

FTIR spectra of silica particles and composite particles were measured using a Nicolet IR 860 spectrometer (Thermo Nicolet, Madison, WI) with a KBR pellet technique. Transmission electron microscope (TEM, JEM 2020CX, JEOL), applying an acceleration voltage of 200 kV, was used to clarify the nanostructure of composites films. The nanocomposite membranes were embedded in an epoxy resin of Epon-812 supplied by SPI. Ultra-thin sections of the nanocomposites with thickness of ~ 70 nm were prepared at −60°C by a ultramicrotome of Ultracut R made by Leica. Carbon was vacuum-evaporated on the thin sections to prevent accumulation of electrons during TEM observation.

RESULTS AND DISCUSSION

Formation of silica/polymer nanocomposite membranes

In general, proton exchange membranes (PEM) are fabricated via solvent casting process. Our silica/polymer nanocomposite membranes were fabricated through bulk curing process similar to bulk mold-compounding (BMC) process. Surface grafting of silica nanoparticles, synthesis of urethane acrylate, copolymerization, stabilization of dispersed silica particles, and urethane bridging took place consecutively and continuously in the same medium.

At the 1st step, highly excess amounts of TDI were added and reacted with silica nanoparticles. And, the reactivity of NCO at *para*-position of TDI is much higher than that of NCO at *ortho*-position of TDI at the room temperature. So, silanol groups onto the silica surface were preferentially reacted with *para*-positioned NCO groups of TDI, whereas *ortho*-positioned NCO groups would remain intact, and most of NCO groups remained unreacted in the solution.[25,26] Consequently, after completion of the 1st step, unreacted TDI molecules and silica nanoparticles having NCO groups onto their surface coexisted in DMSO, respectively. At the 2nd step, 2-HEMA molecules were added and reacted with unreacted TDI molecules and NCO groups bound onto the silica surface at the same time. Through the reaction between OH group of 2-HEMA and NCO group of unreacted TDI or between OH group of 2-HEMA and NCO onto silica surface, formation of free urethane acrylate molecules and introduction of urethane acrylate molecules onto silica particles took place in DMSO medium simultaneously. Since molar ratio of TDI to 2-HEMA was 1 : 1 and NCO groups at *para*-position have higher reactivity, large numbers of *ortho*-positioned NCO groups in TDI could remain unreacted even after completion of 2nd step.

After completion of 2nd step, prepared solution was immersed in water–acetone mixture and centrifuged to separate surface-modified silica particles.

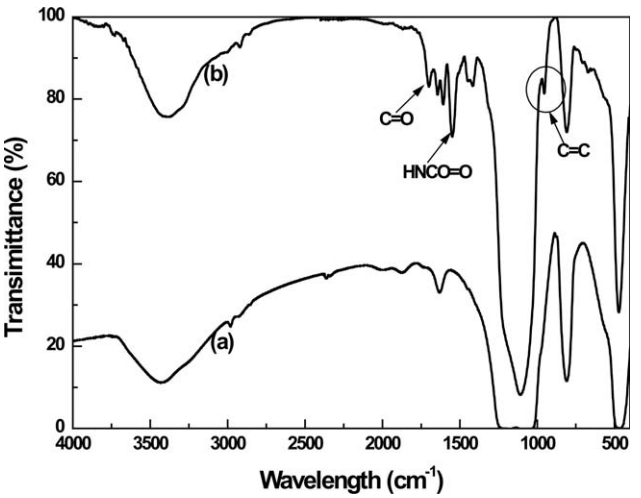

Figure 3 FTIR spectra of silica nanoparticles (Aerosil® 200) and surface-modified silica nanoparticles formed by 2nd step in the fabrication of nanocomposite membrane: (a) silica nanoparticles and (b) surface-modified silica nanoparticles.

Then particles were extracted for overnight with acetone in Soxhlet extractor to remove all chemicals physically adsorbed into the particles. FTIR spectra of palletized particles using KBr were measured and presented at Figure 3. Compared the spectrum of unmodified silica particle, urethane acrylate-introduced silica nanoparticle showed some new absorption peaks at 1720, 1542, and 968 cm^{-1}, which was assigned to carbonyl group, carbamate, and vinly group, respectively. This indicates the introduction of urethane acrylate onto the silica surface.

At the 3rd step, NaSS and UAN were added and mixed the prepared solution at room temperature, then the solution were poured at a mold to carry out curing process. After adding UAN, transparency of the solution increased, indicating the increase of dispersibility of silica nanoparticles in DMSO solution. As reported at our previous papers,[13,14] UAN could increase dispersibility of silica nanoparticles in DMSO, so semitransparent silica/polymer nanocomposite membranes could be fabricated. TEM images of these membranes also showed unmodified silica nanoparticles could be dispersed with 50 nm-sized particles in the polymer membranes.

After completion of 3rd step, semitransparent solutions were converted to semitransparent wall-to-wall membranes. It can be thought that radical initiated copolymerization and urethane bridging took place simultaneously, resulting in formation of membranes. In the course of curing, urethane acrylate groups onto silica surface, urethane acrylate molecules dissolved in DMSO, and NaSS were copolymerized through reaction between their vinyl groups. At the same time unreacted NCO groups in the solution reacted with OH groups of UAN chains. Consequently, silica nanoparticles, urethane acrylate, and UAN molecules were chemically connected with each other by these two different covalent bonding, resulting in formation of wall-to-wall membrane.

Obtained membranes were immersed in water–acetone mixture for 2 days to remove unreacted monomers and have residual NCO reacted water molecules. Then the membranes were placed in 0.5 *M* H_2SO_4 for 2 days, followed by rising and washing with deionized water several times.

Microstructure and proton conductivity

Figure 4 shows TEM image of the composite membranes fabricated with various silica content. The membranes containing 5.89 wt % of the silica particles showed that nanosized silica particles were dispersed in whole matrix. However, the membranes containing 17.27 and 29.45 wt % of silica nanoparticles, showed aggregated and interconnected silica nanoparticles were dispersed in the matrix. This highly aggregated structure of silica nanoparticles at higher silica content can be explained by the increase of interconnection between silica nanoparticles and aggregation of silica nanoparticles. As the silica content increased in the reaction solutions, the amount of introduced vinyl groups onto the silica particles and NCO bridging between OH groups onto silica particles increased, resulting in increase of interconnection between silica nanoparticles. Consequently, interconnected and aggregated silica nanoparticles were dispersed and formed their domains in polymer matrix even in the presence of reactive dispersant, UAN.

Figure 5 shows the proton conductivity of a polymer membrane and silica/polymer nanocomposite membranes prepared at various weight % of silica nanoparticles. All membranes exhibited the proton conductivity a little greater than or equal to 10^{-2} S cm^{-1}. Since all membranes were fabricated using the same amount of NaSS, the membranes have the same ionic contents participating in proton conduction. Even though the membranes were fabricated at various weight % of silica nanoparticles, they showed almost same proton conductivity. So, it can be thought that dispersed silica nanoparticles in the composite membranes did not influence microstructure of hydrophilic domains where protons move through.

As presented in Table II, water uptake of the composite membranes was much lower than that of the membrane containing 0 wt % of silica particles. Since hydrophobic domains of the membranes are formed by TDI, HEMA and hydrophobic segment of UAN chains, it can be thought that the composite membranes (SSUH) and a polymeric membrane (PUSS)

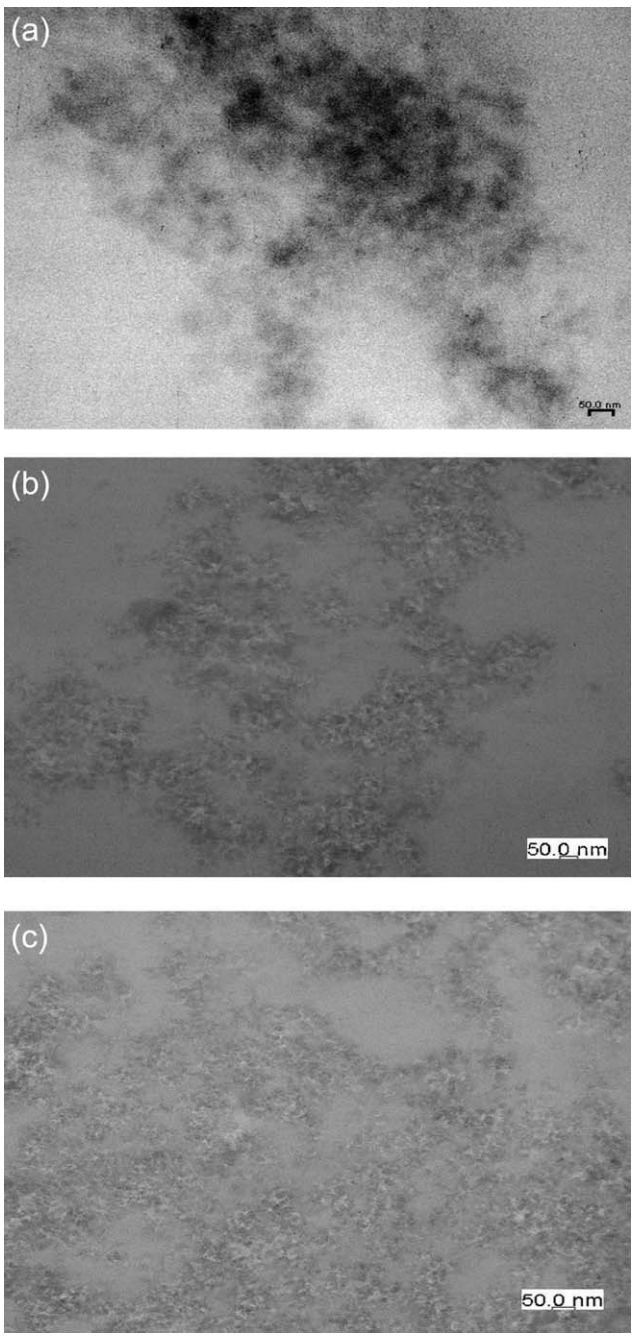

Figure 4 TEM images of silica/polymer nanocomposite membranes: (a) 5.89 wt % of silica nanoparticles, (b) 17.27 wt % of silica nanoparticles, and (c) 29.45 wt % of silica nanoparticles.

have the same chemical structure and the same amount of sulfonic contents. However, PSSU and SSUH membranes showed very different water uptake. That is, PUSS membrane showed 154.7% of water uptake, but the composite membranes showed much lower water uptake (21.96–58.67%). This indicates that water uptake of the membranes was largely decreased by incorporation of silica particles in the polymer matrix regardless of the same sulfonic contents.

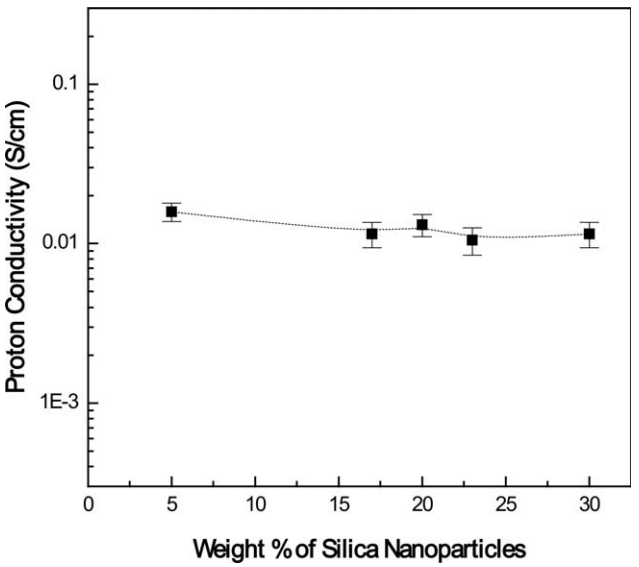

Figure 5 Proton conductivity of silica/polymer nanocomposite membranes as a function of wt % of silica nanoparticles.

In general, proton exchange membranes exhibit the increase of proton conductivity with the increase of water uptake of the membranes, because proton conduction takes place exclusively through water-swollen hydrophilic ionic domains formed by association of ionic groups of the membranes. So, increase of the sulfonic contents in the membranes generally causes the increase of proton conductivity and increase of water uptake, simultaneously. High water uptake of the membranes highly deteriorates their physical properties and performance, so water uptake of proton exchange membrane should be controlled as low as possible. However, reduced water uptake inevitably also causes decreased in proton conductivity. In our system, all membranes have the same sulfonic contents and chemical compositions, so membranes showed the almost same proton conductivity but exhibited very different water uptake. This result indicates that silica nanoparticles dispersed in polymer matrix highly

TABLE II
Water Uptake and Methanol Permeability of Nanocomposite Membranes

Sample	Water uptake (%)	Proton conductivity (S cm^{-1})
PSSU	145.54–164.31 (154.7)[a]	0.0141–0.0174 (0.0149)[a]
SSUH-1035	21.16–23.85 (21.96)[a]	0.0139–0.0180 (0.0158)[a]
SSUH-1100	45.26–52.18 (48.35)[a]	0.0094–0.01354 (0.0115)[a]
SSUH-1125	46.80–52.54 (49.51)[a]	0.0111–0.01525 (0.0131)[a]
SSUH-1150	49.47–56.00 (52.63)[a]	0.0085–0.01262 (0.0105)[a]
SSUH-1200	54.82–62.52 (58.67)[a]	0.0094–0.01359 (0.0115)[a]

[a] Average values.

suppressed swelling of hydrophilic domains by absorbing water molecules without hampering proton conduction.

For comparison of water uptake among the nanocomposite membranes, the composite membranes fabricated using higher silica nanoparticle content showed higher water uptake. This can be interpreted by two reasons. That is, one is lower degree of crosslinking of the membranes and the other is a greater amount of free OH groups of UAN after fabrication process. As mentioned earlier, added TDI molecules reacted with silanol groups of silica particles and OH groups of UAN chains in the course of membrane fabrication. As the silica particle content increase in the reaction composition, the degree of reaction between NCO groups of TDI with silanol group of silica particles increased but degree of reaction between NCO groups of TDI and OH group of UAN decreased. Consequently, interconnection between silica nanoparticles increased but urethane bridging between UAN chains decreased, which caused the decrease in degree of crosslinking of the membranes. In addition, water solubility of polyethylene oxide chain having free OH groups is much higher than that of neat polyethylene oxide chains. At higher silica content, the reaction between NCO groups of TDI and OH groups of UAN chains decreased, so remaining amount of OH groups of UAN chains increased, which results in the increase of hydrophilicity of the membranes.

Thermal and chemical stability of the composite membranes

Figure 6 shows TGA curves of the membranes under a nitrogen purge. All membranes exhibited the first weight loss at 100°C because of the loss of absorbed water. Since all membranes have the same sulfonic acid content, all membrane also showed almost same weight loss at this temperature. The membranes exhibited the 2nd weight loss region between 250 and 400°C, which can be interpreted as loss of sulfonic acid from the desulfonation and the breakage of urethane bonding. The final weight loss above 400°C can be interpreted as the decomposition of polymer main chain.

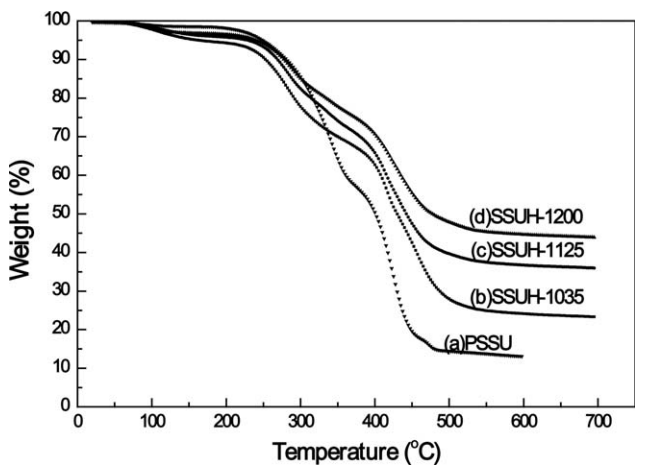

Figure 6 TGA curves of PSSU and SSUH membranes.

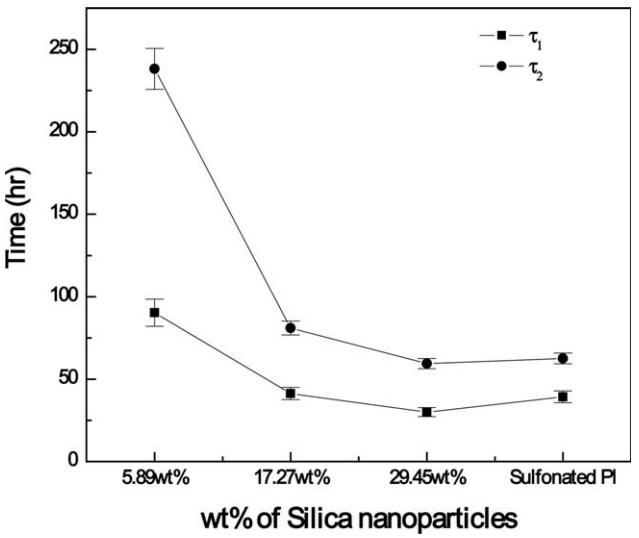

Figure 7 Oxidative stability of the nanocomposite membranes prepared using various amount of silica nanoparticles. *SPI is the abbreviation of sulfonated polyimide.

PSSU membranes prepared without silica nanoparticles showed a very sharp weight loss curve compared to all SSUH nanocomposite membranes. As the silica content increased from 5.89 to 29.45 wt %, the nanocomposite membranes showed smaller amount of weight loss and slower speed of weight loss. These results indicate the dispersed silica particles in polymer matrix highly improve thermal stability of the pristine membrane. The nanocomposite membrane containing 29.45 wt % of silica particles exhibited almost 50% of weight residue even above 700°C.

Figure 7 shows the oxidative stability of nanocomposite membranes measured using Fenton's reagent. The oxidative stability of the membranes was characterized by the elapsed time at which the membranes started to dissolved and dissolved completely in the solution. The membranes fabricated using 5.89 wt % (SSUH-1035) and 17.27 wt % (SSUH-1100) of silica nanoparticles endure for 90 and 40 h, respectively. It took 240 h for SSUH-1035 membrane to be completely dissolved in Fenton's reagent solution, which is much higher oxidative stability compared to oxidative stability of our sulfonated polyimide membranes presented at our previous papers.[20,24] This result indicates silica nanoparticles dispersed in membranes matrix highly increased chemical stability of the organic membranes.

The interesting results is that the composite membranes containing 5.89 wt % of silica nanoparticles showed higher oxidative stability than the composite membranes containing 17.27 and 29.45 wt % of silica particles, even though the composite membranes containing higher amount of silica particles showed higher thermal stability. So, it can be thought that SSUH-1035 (5.89 wt % silica content) membrane has the most dense crosslinked structure and strongest structure of inorganic/organic membrane. As earlier mentioned, SSUH-1035 membrane (5.89 wt % of silica content) showed the lowest swelling ratio in water because of higher degree of crosslinking.

CONCLUSIONS

Inorganic/organic nanocomposite membranes containing very high silica nanoparticle content could be fabricated using *in situ* grafting reaction and reactive dispersion process in the presence of reactive dispersion agent (UAN). Because of synergistic effect of dispersion capability of UAN, surface modification of silica nanoparticles, and chemical reactions between silica nanoparticles and organic reactants, very high contents of silica nanoparticles (17.27–29.45 wt %) could be dispersed or incorporated within organic polymer matrix. Compared to organic membranes having the same chemical composition, all nanocomposite membranes showed better chemical and thermal stability, and water uptake could be also largely reduced by incorporation of silica particles without sacrificing proton conductivity. The nanocomposite membranes showed the best property at optimal silica content (5.89 wt %). That is, SSUH-1035 membrane containing 5.89 wt % of silica nanoparticles showed much reduced water uptake and excellent oxidative stability. This nanocomposite membrane seems promising for the application to PEMFC or DMFC.

References

1. Nolte, R.; Ledjeff, K.; Mulhaupt, R. J Membrane Sci 1993, 83, 211.
2. Kerres, J.; Cui, W.; Disson, R.; Neubrand, W. J Membrane Sci 1998, 139, 211.
3. Sumner, M. J.; Harrison, W. L.; Weyers, R. M.; Kim, Y. S.; McGrath, J. E.; Riffle, J. S.; Brink, A.; Brink, M. H. J Membrane Sci 2004, 239, 199.
4. Bébin, P.; Caravanier, M.; Galiano, H. J Membrane Sci 2006, 278, 35.
5. Honma, I.; Takeda, Y.; Bae, J. M. Solid State Ionics 1999, 120, 255.
6. Honma, I.; Nomura, S.; Nakajima, H. J Membrane Sci 2001, 185, 83.
7. Nunes, S. P.; Ruffmann, B.; Rikowski, E.; Vetter, S.; Richau, K. J Membrane Sci 2002, 203, 215.
8. Kim, D. S.; Park, H. B.; Rhim, J. W.; Lee, Y. M. J Membrane Sci 2004, 240, 37.
9. Kim, Y. M.; Choi, S. H.; Lee, H. C.; Hong, M. Z.; Kim, K.; Lee, H. I. Electochim Acta, 2004, 49, 4787.
10. Mauritz, K. A.; Stefanithis, I. D.; Davis, S. V.; Scheetz, R. W.; Pope, R. K.; Wilers, G. L.; Huang, H. H. J Appl Polym Sci 1995, 55, 181.
11. Miyake, N.; Wainright, J. S.; Savinell, R. F. J Electrochem Soc 2001, 148, A898.
12. Jiang, R.; Kunz, H. R.; Fenton, J. M. J Membrane Sci 2006, 272, 116.
13. Kim, J. Y.; Mulmi, S.; Lee, C. H.; Park, H. B.; Chung, Y. S.; Lee, Y. M. J Membrane Sci 2006, 283, 172.
14. Kim, J. Y.; Mulmi, S.; Lee, C. H.; Lee, Y. M.; Ihn, K. J Appl Polym Sci 2008, 107, 2150.
15. Kim, J. Y.; Shin, D. H.; Ihn, K. J.; Nam, C. W. Macromol Chem Phys 2002, 203, 2454.
16. Kim, J. Y.; Shin, D. H.; Ihn, K. J. J Appl Polym Sci 2005, 97, 2357.
17. Taniguchi, Y.; Shirai, K.; Saitoh, H.; Yamauchi, T.; Tsubokawa, N. Polymer 2005, 46, 2541.
18. Yokoyama, R.; Suzuki, S.; Shirai, K.; Yamauchi, T.; Tsubokawa, N.; Tsuchimochi, M. Eur Polym J 2006, 42, 3221.
19. Lee, C. H.; Park, H. B.; Lee, Y. M.; Lee, R. D. Ind Eng Chem Res 2005, 44, 7617.
20. Lee, C. K.; Park, H. B.; Chung, Y. S.; Lee, Y. M.; Freeman, B. D. Macromolecules 2006, 39, 755.
21. Wu, S.; Qiu, Z.; Zhang, S.; Yang, X.; Yang, F.; Li, Z. Polymer 2006, 47, 6993.
22. Zhong, S.; Liu, C.; Dou, Z.; Li, X.; Zhao, C.; Fu, T.; Na, H. J Membrane Sci 2006, 285, 404.
23. Liu, B.; Kim, D. S.; Murphy, J.; Robertson, G. P.; Guiver, M. D.; Mikhaillenko, S.; Kaliaguine, S.; Sun, Y. M.; Liu, Y. L.; Lai, J. Y. J Membrane Sci 2006, 280, 54.
24. Lee, C. H.; Hwang, S. Y.; Sohn, J. Y.; Park, H. B.; Kim, J. Y.; Lee, Y. M. J Power Sources 2006, 163, 339.
25. Che, J.; Xiao, Y.; Wang, X.; Pan, A.; Yuan, W.; Wu, X. Surface Coating Technol 2007, 201, 4578.
26. Pacard, E.; Brook, M. A.; Ragheb, A. M.; Pichot, C.; Chaix, C. Colloid Surface B 2006, 47, 176.